DOI: 10.1002/cbic.200800280

Influence of a Joining Helix on the BLUF Domain of the YcgF Photoreceptor from *Escherichia coli*

Claudia Schroeder,[a] Karla Werner,[b] Harm Otten,[a] Steffen Krätzig,[a] Harald Schwalbe,[b] and Lars-Oliver Essen*[a]

BLUF-domain-comprising photoreceptors sense blue light by utilizing FAD as a chromophore. The ycgF *gene product of* Escherichia coli *is composed of a N-terminal BLUF domain and a C-terminal EAL domain, with the latter postulated to catalyze c-di-GMP hydrolysis. The linkage between these two domains involves a predominantly helical segment. Its role on the function of the YcgF photoreceptor domain was examined by characterizing BLUF domains with and without this segment and reconstituting them with either FAD, FMN or riboflavin. The stability of the light-adapted state of the YcgF BLUF domain depends on the presence of this joining, helical segment and the adenosine diphosphate moiety of FAD. In contrast to other BLUF domains, two-dimensional $^{1}H,^{15}N$ and one-dimensional ^{1}H NMR spectra of isotope-labeled YcgF-(1–137) revealed large conformational changes during reversion from the light- to the dark-adapted state. Based on these results the function of the joining helix in YcgF during signal transfer and the role of the BLUF domain in regulating c-di-GMP levels is discussed.*

Introduction

Photoreceptors utilize light-sensing chromophores to absorb light. Photon capture triggers conformational changes of the protein, leading to an excited or signaling state. This excited state interacts with downstream pathways, activates a signaling cascade[1] and eventually returns to the ground state, ceasing the signaling stimulus until a new photon is absorbed.

In BLUF (sensors for blue-light-using FAD) domain-comprising photoreceptors, the noncovalently bound chromophore FAD interacts with blue light and initiates a photocycle.[2] BLUF-domain-containing proteins occur in proteobacteria, cyanobacteria and a few eukaryotic organisms. They regulate the catalytic activity of enzymes and second messengers,[3] are involved in photophobic responses[4] and control the expression of photosynthetic genes.[3] Until now, the following proteins with BLUF domains have been characterized: AppA,[5–14] and BlrB[15,16] from the purple bacterium *Rhodobacter sphaeroides*, Slr1694 from the cyanobacterium *Synechocystis* sp.,[17–20] Tll0078 from *Thermosynechococcus elongatus*,[4,17,18,21,22] and PAC from the alga *Euglena gracilis*.[4,23] A characteristic feature of their BLUF domains is the reversible red-shift in UV/Vis spectra after illumination of the dark-adapted state, which corresponds to formation of a signaling state.[7] The red-shift is probably entirely generated by rearrangement of the hydrogen-bonding network between the flavin chromophore and surrounding amino acids.[6,11,13,19,20] Although BLUF photocycles have been intensely studied for AppA, BlrB, Slr1694 and Tll0078, the precise mechanism of light conversion is still under debate. For formation of the light-adapted state, light-driven electron transfer and possibly also proton transfer from a conserved Tyr residue have been discussed. These are followed by hydrogen bond rearrangements, a 180° rotation of a conserved glutamine, and transient recombination of a radical pair.[13,16,24–28] Recently, a novel mechanism was proposed on the basis of quantum-chemical calculations that predicted a light-driven tautomerization of the conserved glutamine residue.[29]

The YcgF photoreceptor from *Escherichia coli* is another spectroscopically characterized BLUF domain that exhibits the characteristic red-shift upon illumination.[30–32] Here, an EAL domain is C-terminally linked as an effector region to the BLUF domain. Such EAL domains have been shown to exhibit phosphodiesterase activity[33,34] against cyclic-di-guanosine monophosphate (c-di-GMP), a global second messenger used by bacteria to control multicellular behavior.[35–38] Accordingly, it was proposed that YcgF might function as a blue-light-regulated phosphodiesterase (Blrp) and control biofilm formation.[30,38]

Signal transmission within many biological receptors crucially depends on α-helical segments that join receptor and effector domains.[39–41] For example, in phototropins, a single α-helix (Jα) joins the photoreceptive LOV2 domain to a protein kinase effector domain. NMR spectroscopy showed that the Jα-helix is associated with the PAS fold of the LOV domain in the dark-adapted state and displaced in the light-adapted state.[40] Apparently, light-induced local structural changes around the FAD chromophore trigger the nonlocal disruption of the interac-

[a] *C. Schroeder, H. Otten, S. Krätzig, Prof. Dr. L.-O. Essen*
Department of Chemistry and Biochemistry, Philipps-Universität
Hans-Meerwein-Strasse, 35032 Marburg (Germany)
Fax: (+49) 6421-28-22191
E-mail: essen@chemie.uni-marburg.de

[b] *Dr. K. Werner, Prof. Dr. H. Schwalbe*
Institute for Organic Chemistry and Chemical Biology
Center for Biomolecular Magnetic Resonance (BMRZ), Johann Wolfgang Goethe-Universität
Max-von-Laue-Strasse 7, 60438 Frankfurt am Main (Germany)

Supporting information for this article is available on the WWW under http://www.chembiochem.org or from the author.

tions between the LOV domain surface and its C-terminal Jα-helix followed by activation of this LOV kinase. A similar joining helix is predicted by secondary-structure analysis to link the BLUF and EAL domains of the *E. coli* photoreceptor YcgF. In the following, its potential influence on the properties of the YcgF BLUF domain, such as flavin binding, photochemistry and overall conformational state, have been examined.

Results

YcgF BLUF domains

YcgF (403 aa, molecular mass 45.3 kDa, Swiss-Prot entry P75 990) is composed of an N-terminal BLUF photoreceptor domain (L2–L97) and a C-terminal EAL domain (P145–K403). EAL domains adopt a TIM barrel-like fold as exemplified by the crystal structure of the YkuI dimer from *Bacillus subtilis* (PDB ID: 2BAS) and possess phosphodiesterase activity against cyclic-di-GMP, a bacterial second messenger.[33,34] Both domains of YcgF are connected by a linker region (R98–I144) that is predominantly α-helical as judged by secondary structure predictions utilizing the Jpred server (http://www.compbio.dundee.ac.uk/~www-jpred/). A comparison with available 3D structures of BLUF domains that harbor additional peptide stretches beyond the C-terminal end of the canonical BLUF fold indicated that only the putative helical segment R124–E137 is a candidate for a unique linker helix between the BLUF and EAL domains of YcgF (Figure 1).

Expression, reconstitution and purification

To examine the role of the putative joining helix in YcgF, the BLUF domains YcgF-(1–113) and YcgF-(1–137) were produced as insoluble inclusion bodies, refolded and reconstituted by dialysis. Developed as a strategy to obtain large quantities of soluble, untagged BLUF photoreceptors from inclusion bodies, this method provided the YcgF-(1–113) and YcgF-(1–137) BLUF domains homogenously reconstituted with flavin chromophores such as FAD, FMN or riboflavin in yields of approximately 70 and 115 mg protein per liter culture, respectively. During refolding of the YcgF BLUF domains, an excess of the respective flavin chromophore was added. By using optimized

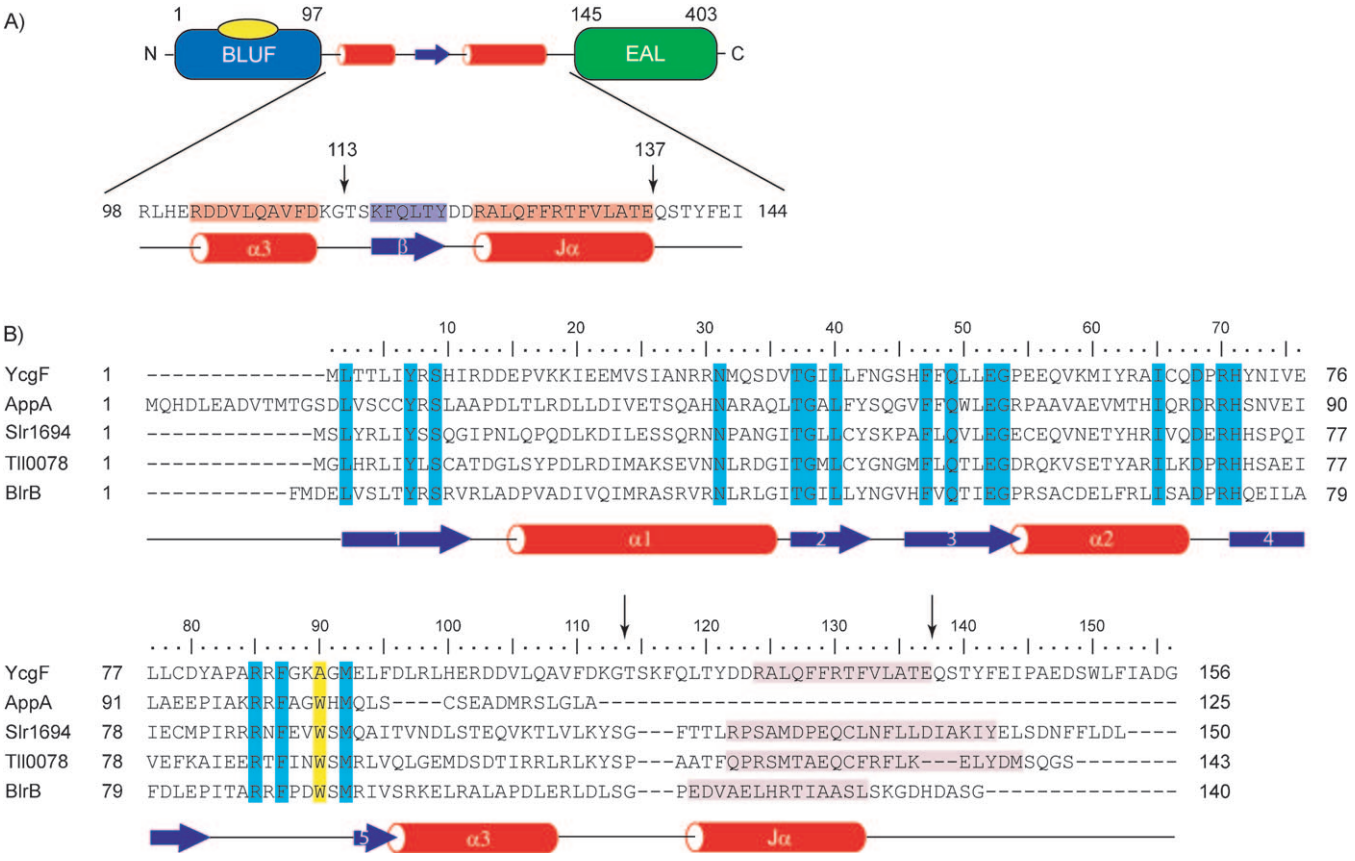

Figure 1. Domain arrangement of *E. coli* YcgF and multiple sequence alignment of BLUF domain containing photoreceptors. A) Secondary structure elements of the linker region were predicted with the Jpred server (http://www.compbio.dundee.ac.uk/~www-jpred/). B) Multiple sequence alignment as generated by ClustalW (http://www.ebi.ac.uk/Tools/clustalw/). Shown secondary structure elements are according to the structure *of R. sphaeroides* BlrB (2BYC) that belongs to the same subfamily as *E. coli* YcgF.[15] The secondary structure elements are shown in red cylinders (α-helices) and blue arrows (β-sheets). The black arrows point to the C-terminal amino acid residue of the analysed YcgF BLUF domains. The Jα-like helices in the structures of BLUF domains are highlighted in pink, one of which (YcgF) was predicted by the Jpred server (http://www.compbio.dundee.ac.uk/~www-jpred/). Residues conserved in all sequences in the alignment are highlighted in light blue and the position of the conserved tryptophan, which is missing and substituted by Ala 90 in YcgF is highlighted in yellow. YcgF of *E. coli* (P75 990); BlrB of *R. sphaeroides* (Q3IYE4); AppA, a 1–125 truncated fragment, of *R. sphaeroides* (Q53 119); Slr1694 of *Synechocystis* sp. PCC 6803 (P74 295); Tll0078 of *T. elongatus* BP-1 (Q8DMN3).

molar chromophore/protein ratios (FAD: 7.5, FMN, riboflavin: 15), 74–81% of the YcgF-(1–113) BLUF domain and up to 100% of YcgF-(1–137) were refolded and reconstituted by this procedure (Table 1). After refolding, the BLUF domains were further purified by size-exclusion chromatography (Figure 2A and B). The light-adapted BLUF domain without joining helix, YcgF-(1–113), eluted at an apparent molecular mass of 59 kDa. Given its molecular mass of 13.2 kDa, a tetrameric or pentameric state is expected for this protein. In contrast, the light-adapted BLUF domain comprising the joining helix, YcgF-(1–137), eluted as a dimer at an apparent molecular mass of 31 kDa. Accordingly, the absence of the Jα-helix might trigger additional, unspecific interactions in light-adapted YcgF-(1–113) by unmasked surface regions. This unmasking could allow the YcgF-(1–113) BLUF domain to assemble into oligomers similar to the pentameric rings formed by stand-alone BLUF domains such as Slr1694 or Tll0078.[22,42] The presence of the joining region sterically interferes with higher-order oligomerisation found for stand-alone BLUF domains and could enforce a similar dimeric state as for the BLUF domains in AppA.[13,14,43] Although recombinant full-length YcgF was initially reported to form predominantly monomers,[30] dimerization was observed for its light-adapted state by pulsed laser-induced transient grating techniques.[31]

Table 1. Maximum yields after reconstitution by refolding with different flavin chromophores and protein/chromophore ratios of purified YcgF BLUF domains.

	Yield [%]	Protein concentration [mM]	Chromophore concentration [mM]	Calculated ratio
YcgF-(1-137)/FAD	99.0	0.860	0.971	1:1.13
YcgF-(1-137)/FMN	96.8	1.490	1.470	1:0.98
YcgF-(1-137)/Rib	96.8	0.767	0.656	1:0.86
YcgF-(1-113)/FAD	81.3	0.778	1.070	1:1.37
YcgF-(1-113)/FMN	73.9	0.636	0.680	1:1.07
YcgF-(1-113)/Rib	74.5	0.350	0.310	1:0.89

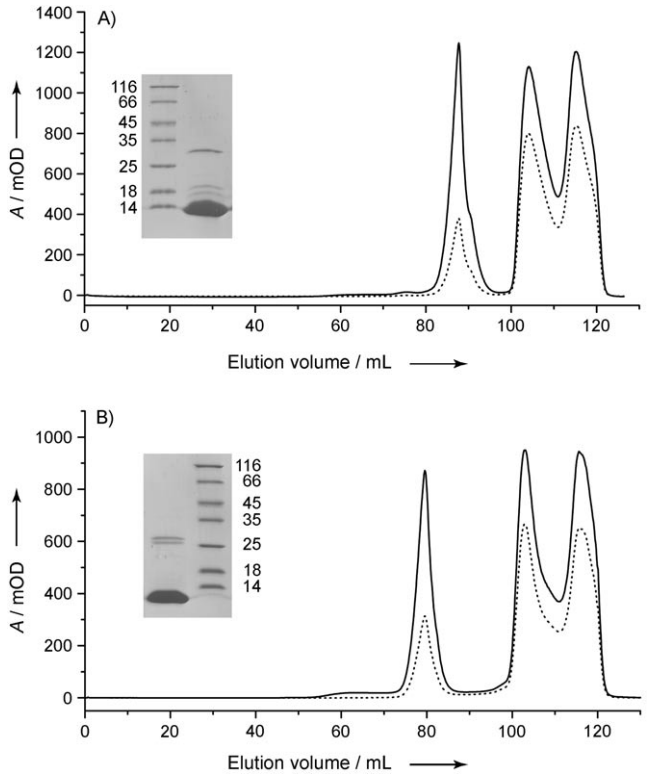

Figure 2. Size exclusion chromatography of *E. coli* YcgF BLUF domains reconstituted with FAD. The chromatography utilized a Superdex 200 XK 16/70 column; detection occured at 280 nm (——) and 445 nm (····). A) The applied YcgF-(1–137)/FAD was eluted after 87.7 mL with an OD_{445}/OD_{280} ratio of 0.31 and B) YcgF-(1–113)/FAD was eluted after 79.6 mL with an OD_{445}/OD_{280} ratio of 0.36. The double peak in the range of 100 to 120 mL represents the elution of the surplus FAD cofactor. The inlays show 15% SDS PAGE gels of the refolded and purified YcgF BLUF domains. Numbers left and right respectively correspond to the molecular mass in kDa.

To analyze whether the refolding procedure yielded homogeneous BLUF photoreceptors, chromophore/protein ratios were determined. Proteins were heat denatured by using a previously described protocol, [44] and corrected flavin extinction coefficients were applied. Ratios of approximately 1:1 were detected (Table 1), showing only small differences for the different flavin chromophores. The ease with which YcgF BLUF domains could be reconstituted with different flavins indicates that the riboflavin moiety is sufficient for the formation of flavin-bound YcgF photoreceptor domains and explains why functionally overproduced BLUF domains were found to comprise nonstoichiometric mixtures of FAD, FMN and riboflavin.[9,15,16,23,45,46]

UV/Vis spectroscopy

Independent of the incorporated flavin species, the dark-adapted UV/Vis spectra of both YcgF BLUF domains show the typical absorption bands of the oxidized flavin chromophore with maxima at 384 nm and 456–461 nm (Figure 3). The second maximum differs slightly depending on the presence or absence of the C-terminal Jα-helix. Upon illumination, its peak position is red-shifted by approximately 8 nm for YcgF-(1–113) and 4 nm for YcgF-(1–137) (Supporting Information). A shoulder in the range of 470 nm to 500 nm is observed for the dark- and light-adapted states. These features are similar to those of other BLUF domains, for example, from AppA, Slr1694 and YcgF (Blrp).[6,10,15,19,20,30,32] Figure 4A shows a reversible light-to-dark conversion that exhibits five isosbestic points at approximately 375, 410, 465, 474 and 487 nm. The YcgF BLUF domain's difference spectra (Figure 4B) is qualitatively similar to that of AppA and intact YcgF[6,30,32] and contains minima at of 341, 379, 428, and 481 nm and maxima at 396, 469, and 503 nm (Supporting Information).

Time courses for the decay of the light-adapted state were measured at 292 K and 503 nm by using both YcgF BLUF domain variants reconstituted with either FAD, FMN or riboflavin. The different dark recovery rates shown in Table 2 and in the Supporting Information were calculated by assuming monoexponential decay. The resultant half-lives for the light-adapted states of the examined YcgF BLUF domains differ depend-

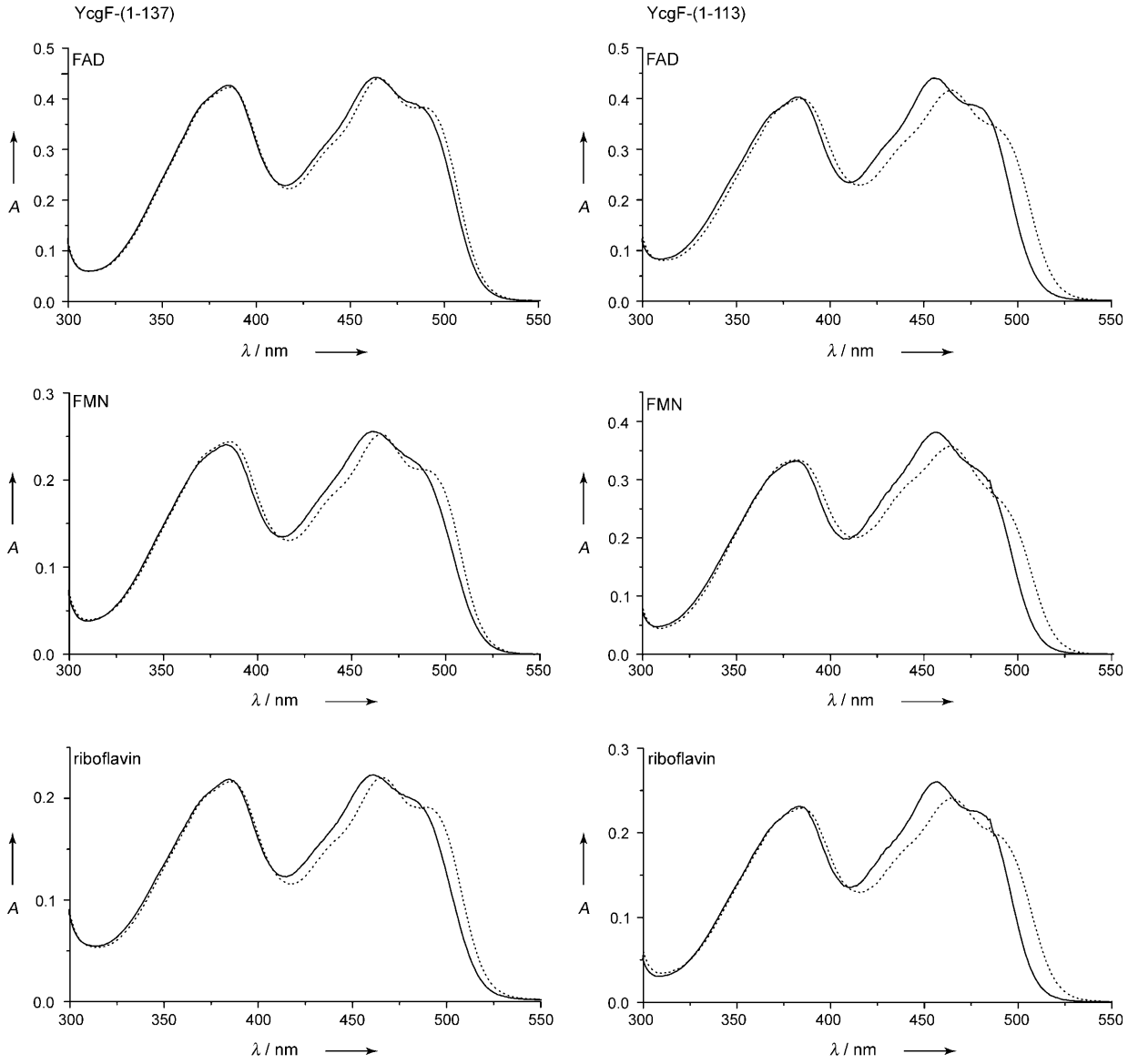

Figure 3. UV-visible absorption spectra of the dark-adapted (——) and light-adapted (····) YcgF BLUF domains YcgF-(1–137) and YcgF-(1–113) reconstituted with FAD, FMN and riboflavin. Both BLUF domain variants were dissolved in Tris/HCl (20 mM, pH 8.0) buffer containing NaCl (200 mM). Data were collected at 18 °C.

ing on the presence of the joining helix and their respective flavin chromophore. The YcgF-(1–137) BLUF domain's decay kinetics are generally slower than those of YcgF-(1–113); this suggests a stabilizing effect of the additional Jα-helix on the light-adapted state. In YcgF-(1–137), the light-adapted state decayed with half-lives of 23.8 min, 14.7 min and 14.4 min for FAD, FMN and riboflavin, respectively. Apparently, the adenosine moiety of FAD causes an additional stabilization of the light-adapted state in dimeric YcgF-(1–137), but not in the tetra-/pentameric YcgF-(1–113) variant. Nevertheless, the kinetics of the two YcgF BLUF domain variants resemble those observed for the BLUF domain of AppA ($t_{1/2}=15$ min)[7] and full-length YcgF ($t_{1/2}=5.22$ min),[7,30] but are clearly slower than those reported by Hasegawa et al., for YcgF and YcgF-(1–148) ($t_{1/2}=2.16$ min)[32] and for the stand-alone BLUF domains of Slr1694 ($t_{1/2}=5$ s),[20] BlrB ($t_{1/2}=5$ s)[15] and Tll0078 ($t_{1/2}=5$ s).[21]

CD spectroscopy

The CD spectra of YcgF-(1–113) (Figure 5A) and YcgF-(1–137) (Supporting Information) present a similar mixture of α-helices and β-sheets with approximate ratios of 60 to 40% and 65 to 35%, respectively, that resemble the predicted secondary structure content. The CD spectra are independent of the flavin cofactor incorporated into the YcgF photoreceptor, indicating that FMN and riboflavin lacking the AMP or ADP moiety do not induce observable changes in the secondary structure. Both YcgF BLUF domains show cooperative unfolding when ir-

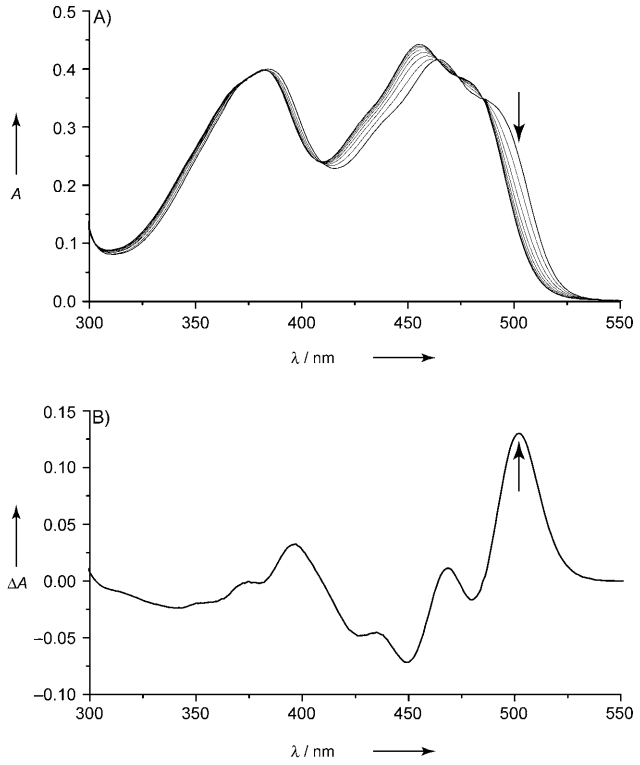

Figure 4. Light–dark conversion and difference spectra of the YcgF BLUF domain. A) UV-visible absorption spectra of the light–dark conversion and B) light minus dark difference spectrum of YcgF-(1–113) reconstituted with FAD. The black arrows marked the wavelength used for determining the dark recovery. The BLUF domain was dissolved in Tris/HCl (20 mM, pH 8.0) buffer containing NaCl (200 mM). Data were collected at 291 K.

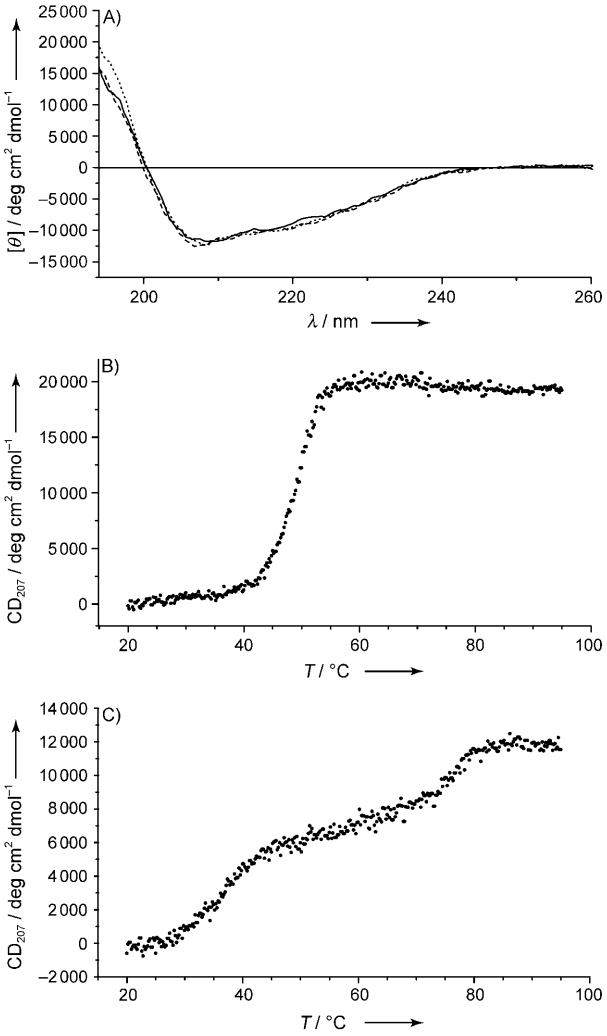

Figure 5. CD-spectroscopic analysis of *E. coli* YcgF BLUF domains. A) CD spectra of YcgF-(1–113) reconstituted with FAD (——), FMN (····) and riboflavin (-----) and melting curves of B) YcgF-(1–137) and C) YcgF-(1–113) reconstituted with the native chromophore FAD. The second transition at 78 °C could indicate the loss of FAD from the denatured state of YcgF-(1–113) as previously reported for other flavoproteins.[67,68] The BLUF domains were dissolved in Tris/HCl (2 mM, pH 8.0) buffer containing NaCl (20 mM). CD data were collected at 20 °C and averaged, while melting curves were recorded at 207 nm from 20 °C to 95 °C.

Table 2. Half-lives of both YcgF BLUF domains reconstituted with FAD, FMN and riboflavin. The BLUF domains were dissolved in Tris/HCl (20 mM, pH 8.0). Data were collected at 292 K.

	$t_{1/2}$ [min]
YcgF-(1-137)/FAD	23.8 ± 5.4
YcgF-(1-137)/FMN	14.7 ± 4.8
YcgF-(1-137)/Rib	14.4 ± 2.0
YcgF-(1-113)/FAD	5.4 ± 1.6
YcgF-(1-113)/FMN	9.7 ± 3.7
YcgF-(1-113)/Rib	4.1 ± 2.7

reversibly heat denatured at 95 °C (Figure 5B and C). The *E. coli* BLUF domain YcgF-(1–137) was unfolded with melting temperatures of 47–49 °C. Only a slight increase of ~1 °C was observed, if FMN or FAD reconstituted BLUF domains were used instead of riboflavin. The YcgF-(1–113)/FAD BLUF domain presented two transitions at 37 and 78 °C (Figure 5C), whereas with FMN and riboflavin only one melting temperature at 42 or 38 °C, respectively, was found. In addition to UV/Vis kinetics and size-exclusion chromatography these results indicate that the C-terminal Jα-helix affects the preceding BLUF domain not only in its photochemical characteristics but also in terms of stability.

NMR spectroscopy

One-dimensional ^{1}H NMR spectra of the light- and dark-adapted states of YcgF-(1–137) reconstituted with FMN, shown in Figure 6A, possess excellent chemical-shift dispersion over the entire spectral range, including a number of strongly downfield- and upfield-shifted peaks. In detail, the −1.4 to 0.6 ppm spectral region shows a number of resolved, but closely spaced methyl resonances, observed for both the light- and dark-adapted YcgF BLUF domain. Upfield-shifted methyl resonances are generally the result of tertiary interactions such as ring current effects derived from neighboring aromatic residues in close spatial proximity to NMR-active nuclei.[6,47–49] Excitation with blue light caused strong shifts in peak positions, relative intensities and overall spectral topology (Figure 6A and C). The changes include a number of resonances at −0.2

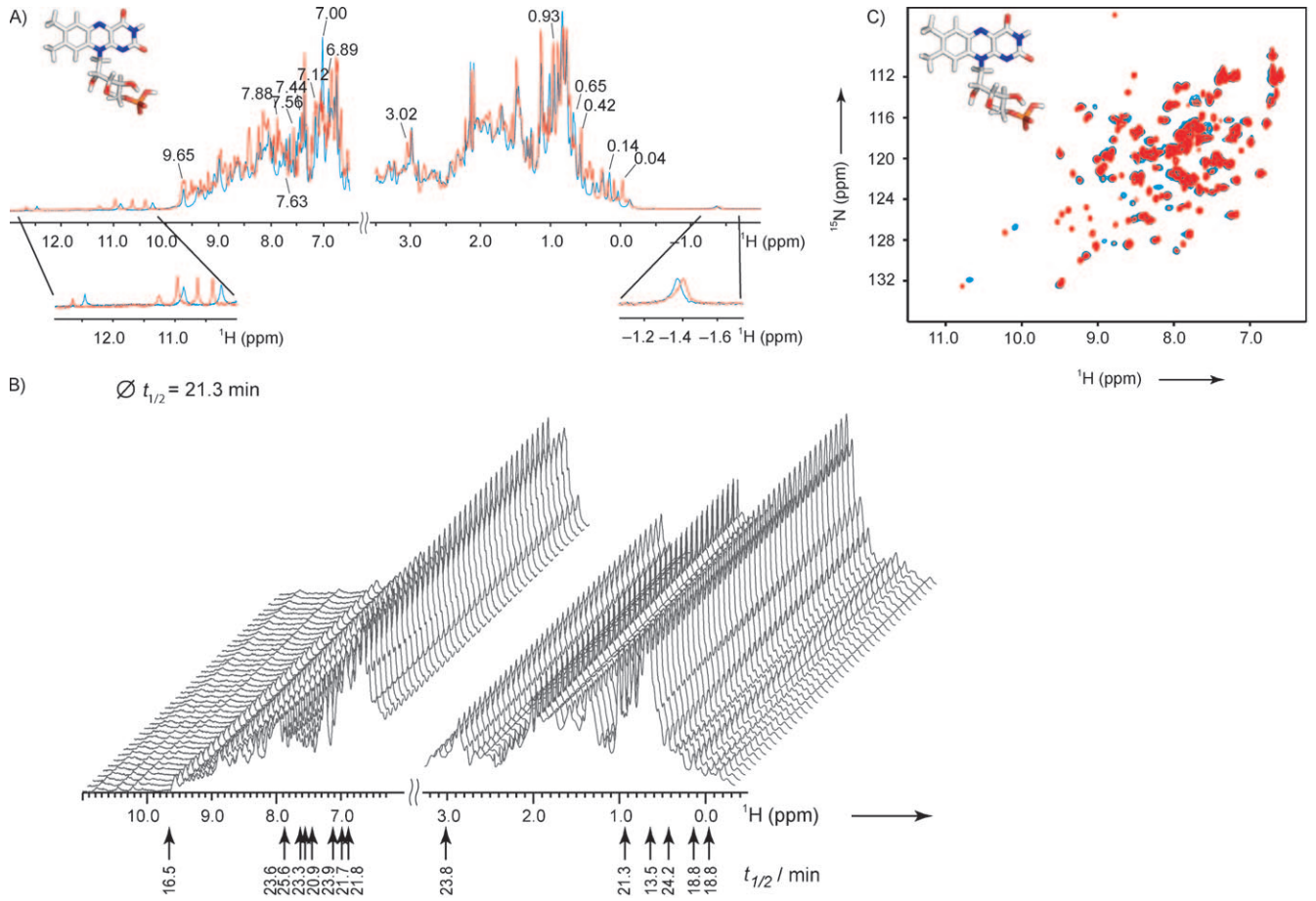

Figure 6. NMR spectra of *E. coli* BLUF domain YcgF-(1–137) reconstituted with FMN recorded under dark- (blue) and light-adapted (red) conditions and of the dark adaptation. A) In the ^{1}H NMR, the downfield and upfield shifted regions are separately displayed. B) Stack plot ^{1}H detected representations recorded after illumination. Spectra were acquired on a Bruker 800 MHz spectrometer using protein (200 μM) in Tris/HCl (20 mM) and NaCl (1 M) at pH 8.0 and 291 K. The black arrows indicate the channels from which the respective measured half-life were delineated. C) $^{1}H,^{15}N$ HSQC spectra were recorded at 600 MHz, 291 K using protein (700 μM) dissolved in Tris/HCl (20 mM), NaCl (1 M), pH 8.0.

to 0.6 ppm, pointing out that the protein environment in the vicinity of these specific methyl groups has been rearranged after illumination. While the $^{1}H,^{15}N$ HSQC spectra contain only two thirds of the expected resonances, including many relatively broad ones caused by high flexibility on an intermediate NMR timescale indicative for millisecond dynamics, significant differences between the light- and the dark-adapted states were observed. In contrast to the HSQC spectra of AppA[5] and BlrB,[15] which showed rather few and mostly small chemical-shift changes upon light excitation, a much larger fraction of peaks are perturbed by illumination of the YcgF BLUF domain. After a certain time period, the original dark spectrum was regenerated without observable degradation, thus establishing the reversibility of these changes at the protein level. No differences were observed when comparing spectra of YcgF-(1–137) reconstituted with either FMN or FAD. Time-dependent ^{1}H NMR spectra of the YcgF-(1–137)/FMN dark adaption were recorded at 291 K showing a half-life of 21.3 min on average (Figure 6B). This value is a mean of at least a dozen decaying and increasing signals that originate from different regions of the spectra. Interestingly, half-lives as determined from these different signals were found to differ significantly from each other. The signals varied from 13.5 to 25.6 min, indicating a complex light–dark conversion process consistent with previous findings.[50,51]

By recording ^{31}P NMR spectra at 291 K, the kinetic behavior of chromophore signals upon illumination was investigated. Figure 7A presents ^{31}P NMR spectra of the BLUF domain YcgF-(1–137) reconstituted with FMN and FAD. Upon illumination, clear upfield shifts for the single phosphate group of FMN as well as for both phosphate groups of FAD of approximately 0.1 ppm were observed. This chemical shift difference allowed the extraction of the intensities of upcoming and decaying signals. Due to the excellent signal-to-noise ratio, a time resolution of 2–3 min could be achieved, which was identical to the resolution of the ^{1}H-detected kinetic experiments. Extraction of the intensities and fitting with mono-exponential functions yielded half-lives of approximately 18–21 min for YcgF-(1–137) reconstituted with either FAD or FMN. These half-lives are similar to the decay rates obtained by the averaged ^{1}H NMR data at the given temperature (Figure 7C). The observed differences are within the error of the experiment. Overall, the NMR data

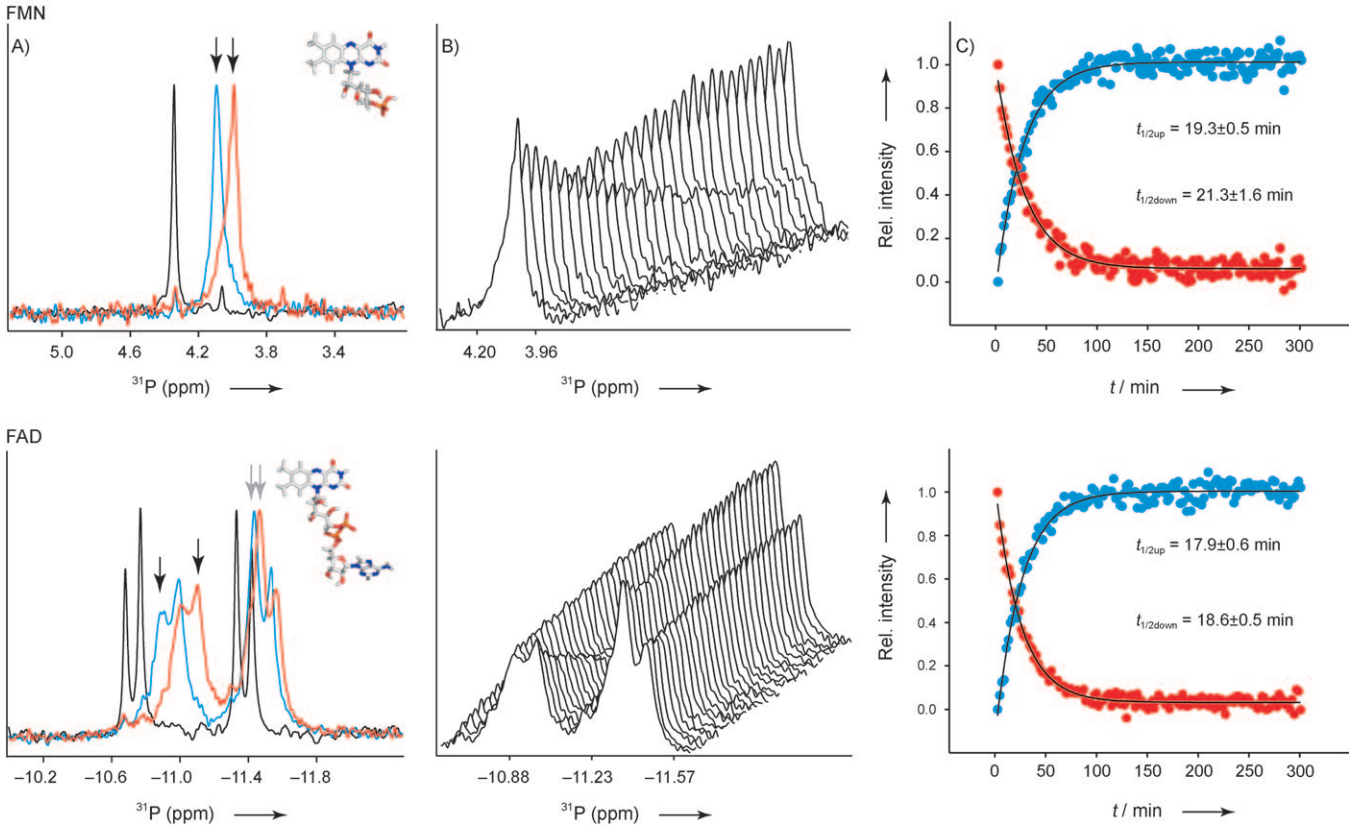

Figure 7. ^{31}P NMR spectra and dark recovery rates of the YcgF-(1–137) BLUF domain reconstituted with FMN and FAD. A) First and last increment of a ^{31}P detected pseudo 2D experiment recorded after illumination. The dark- and light-adapted states are shown in blue and red, respectively, and the free ligands are represented in black. The NMR signals arising from two ^{31}P atoms in FAD are split by scalar ^{2}J(P,P) coupling constant leading to four NMR lines in the experiments for free and bound FAD. B) Stack plot representations of the dark adaptation of the *E. coli* BLUF domain YcgF-(1–137) respectively; in each case the first 32 data points are shown and C) examples for normalized and fitted signal intensities. The positions where the intensities were extracted for the representation are indicated in A) with black arrows. For FAD, $t_{1/2}$ calculations, the intensities highlighted with grey arrows were also considered. The obtained $t_{1/2}$ values are the result of two individual experiments plotted as monoexponential decays over a period of 300 min. Spectra were recorded on a 500 MHz Bruker spectrometer equipped with a QF-HP cryogenic probe at 291 K and 1.5–2.0 mM protein concentration.

are highly consistent with the respective visible light kinetics discussed above, except for the 1.4-fold slower dark conversion time of YcgF-(1–137)/FMN.

Temperature dependence of light–dark-conversion

The half-lives of the YcgF-(1–137)/FMN BLUF domain were recorded by using UV/Vis and NMR spectroscopy between 280 and 297 K in order to study the temperature dependence of the dark recovery rate. Stepwise temperature reduction notably decreases the rate of light–dark conversion, thus suggesting that reversion to the dark state occurs more rapidly at higher temperatures. The logarithm of the time constants versus the inverse temperature was plotted in an Arrhenius plot (Figure 8). The activation energy obtained from the linear fit of the NMR data gave a value of $\Delta E_A = 89\ kJ\,mol^{-1}$. The higher value of $109\ kJ\,mol^{-1}$ obtained from UV/Vis data using the same protein might result from the unavoidable repeated light exposure at 503 nm during the photometric measurements (Table 3). This activation energy is similar to the $\Delta E_A = 81\ kJ\,mol^{-1}$ observed for the Tll0078 BLUF domain.[21] This high activation energy together with the ^{1}H proton and ^{1}H,^{15}N

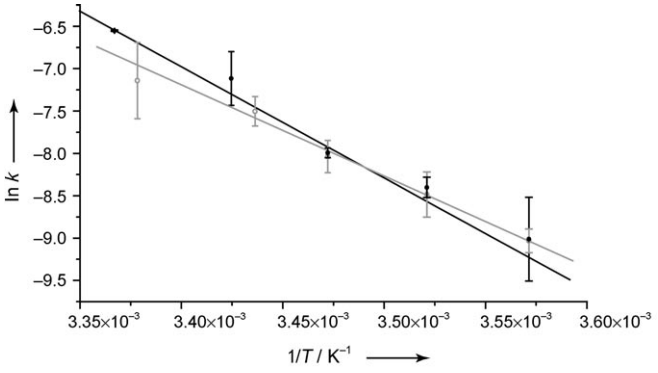

Figure 8. Arrhenius plots including error bars of the dark-state recovery of YcgF-(1–137) reconstituted with FMN. Kinetics were recorded by UV/Vis (-●-) and NMR (-○-) spectroscopy in Tris/HCl (20 mM, pH 8.0). Every UV/Vis measured half-life at 503 nm was measured at least three times and averaged before plotting. The half-lives at 280 K were measured seven times due to a wide divergence. Every NMR-determined time constant is the average of at least 12 decaying and increasing signals at a given temperature. At 288 K two kinetic experiments were carried out, averaged and included in the calculation of E_A. Kinetics were recorded using 30 μM to 75 μM protein for UV/Vis and 300 μM protein and at 600 MHz for NMR spectroscopic measurements.

Table 3. Half-lives determined by UV/Vis and NMR spectroscopy of YcgF-(1–137) reconstituted with FMN. Every NMR determined half-life and time constant is the average of at least twelve decaying and increasing signals at a given temperature. The BLUF domain was dissolved in Tris/HCl (20 mM, pH 8.0).

T [K]	UV/Vis half-life [min]	NMR half-life [min]	NMR t_{min}, t_{max} half-lives [min]
297	8.1 ± 0.1	–	–
296	–	15.9 ± 6.9	6.0 to 27.6
292	14.7 ± 4.8	–	–
291	–	21.2 ± 3.2	13.5 to 25.6
288	34.3 ± 2.0	37.1 ± 3.3	28.9 to 46.8
284	51.7 ± 6.3	57.8 ± 14.1	30.5 to 78.8
280	107.3 ± 46.2	97.6 ± 13.1	76.2 to 119.5
E_A [kJ mol^{-1}]	108.8 ± 3.7	89.3 ± 11.9	

HSQC spectra indicate that distinct changes in the protein structure occur during dark recovery.[10,19–21,52,53]

Discussion

Chromophore–protein interactions

Previous BLUF domain preparations often suffered from a heterogeneous mixture of flavin cofactors when BLUF domains were overexpressed in soluble form.[9,15,16,23,30,45,46] Our refolding procedure of YcgF BLUF domains from inclusion bodies allowed the deliberate incorporation of various flavin chromophores independent of the presence of a C-terminal-joining α-helix. Using this system we first analyzed whether the non-isoalloxazine parts of FAD or putative interactions between the joining helix and the YcgF BLUF domain affected its photochemical behavior. Major differences were not observed for the overall photochemical characteristics when comparing either in vitro and in vivo reconstituted YcgF BLUF domains[30,32] or BLUF domains with and without C-terminally attached Jα-helix. The photochemical properties were also not significantly influenced by the chemical identity of the flavin chromophore as reported for the *R. sphaeroides* AppA BLUF,[9,11] *E. gracilis* PACα F2[23] and the *Avena sativa* LOV2 domains.[54] Accordingly, the observed protein-to-chromophore ratios, the refolding yields or the red-shifts of light-adapted flavin chromophores were not found to depend on the chosen flavin species. Most of the associated structural changes of the YcgF BLUF domain hence take place at the flavin isoalloxazine ring, and neither the adenosine monophosphate moiety nor the phosphate group of FAD is required for formation of the signaling state.

However, the dark recovery rates of YcgF BLUF domains measured by UV/Vis spectroscopy were keenly influenced by the flavin chromophore's nature, contrary to what is observed for AppA[9] and PACα F2.[23] In the absence of a joining helix, FMN appears to interact optimally with the signaling state of the YcgF BLUF domain as represented by the rather large half-life of its light-adapted state of 9.7 min, which is 1.8- and 2.4-times larger than for FAD and riboflavin, respectively. In this case, where the Jα-helix is missing, the phosphate group might interact via salt bridges with the YcgF BLUF photoreceptor as described for AppA[13] and the LOV2 domain.[54,55] Quite contrary to this, in the presence of the Jα-helix, the light-adapted state of the BLUF domain is mostly stabilized if bound to FAD. This specific stabilization might arise either from the dimeric association of the BLUF domain, which is more meaningful for the situation in the intact YcgF photoreceptor than the tetra-/pentameric state of the stand-alone YcgF domain, or from an indirect interaction across the entire YcgF BLUF domain between the C-terminal Jα helix and the jutting AMP moiety. Crystal structures for the AppA[45] and BlrB BLUF domains have shown that the AMP moiety has an outward orientation,[15] when the ribityl side chain and the phosphate group of the chromophore point towards the surface of the respective BLUF domain. Therefore, FAD's AMP moiety is not necessary for *E. coli* YcgF to undergo its photocycle, but it is affected by the structural context of the BLUF domain[15] and can hence contribute to the stabilization of the light-adapted BLUF domain in the intact photoreceptor protein.

The YcgF BLUF domain and the C-terminal Jα-helix

For NMR studies, only the YcgF BLUF domain including the C-terminal Jα-helix was used since the BLUF domain without this joining region adopted a higher oligomeric state and was not tractable for NMR experiments due to its large molecular mass. According to one-dimensional ^{1}H and two-dimensional ^{1}H,^{15}N NMR spectroscopy, the BLUF domain with C-terminally attached Jα-helix undergoes global structural changes between its dark- and light-adapted states. Similar broad conformational changes in the LOV2 domain of plant phototropins were shown to correlate with distinct conformations of the light- and dark-adapted states.[40] Here, a reorientation of the C-terminal Jα-helix during the formation of the light-adapted state was delineated that was crucial for inter-domain signal transfer.[40,50,56] Unfortunately, the complete solution structure of the *E. coli* YcgF BLUF domain could not be determined due to a lack of one third of the expected backbone amide resonances in the ^{1}H,^{15}N NMR spectra.

Unlike the YcgF BLUF domain, many other BLUF domains exhibit only minor structural changes upon light–dark conversion. The AppA BLUF domain without an analogous C-terminal α-helix shows only small changes between light- and dark-adapted states according to HSQC NMR spectroscopy.[5] Similarly, the LOV2ΔJα domain lacking the joining helix displays only minor peak relocations in ^{1}H, ^{15}N NMR spectra of its light- and dark-adapted states.[40] Analogous results were obtained from NMR spectroscopy for the AppA and BlrB BLUF domains, which included either a C-terminal extra-domain region or a helical segment, and for a mutant of LOV2 where the interface between the LOV domain and the Jα-helix was disrupted.[56] [6,15] In all these cases, the C-terminal extensions do not apparently interact with the BLUF core or show significant changes upon illumination of the ground state.

The observed differences for light–dark conversion could correlate with a conserved tryptophan, existent in most BLUF domains, but replaced by alanine in YcgF. In other BLUF domains, the conserved Trp residue is part of the so-called non-productive electron transfer pathway[25] and might participate in the light-dependent formation and breakage of a hydrogen bond to Gln63 during the photocycle.[57] Furthermore, the flip of the indole ring from an inward to an outward orientation during dark–light conversion might transmit conformational changes around the chromophore to the protein surface. Its absence in the YcgF BLUF domain implies that the observed global conformational changes of this BLUF domain might take an alternative route to transmit structural changes to the surface.

Overall, the YcgF BLUF domain appears to show a similar light-triggered conformational change for its Jα-helix like the LOV2 domain. Like the latter, in which additional ^{2}H-exchange and limited proteolysis experiments were performed,[40] widespread chemical dispersion in both the light- and dark-adapted states suggest that the Jα-helix moves without disrupting the BLUF domain fold of YcgF. Furthermore, the Jα-helix stabilizes both the *E. coli* YcgF BLUF domain and its light-adapted state and influences its sensor properties, as reflected by higher refolding yields, higher melting points, decreased red-shifts of the light-adapted state and slower dark-recovery rates. In addition to the light-induced structural changes seen in LOV2 domains, light-induced structural changes at the extensions of photoreceptor domains might be a general theme, as they were observed for the so-called DAS motive of *A. thaliana* cryptochrome 1[58] and a N-terminal helical segment of the photoactive yellow protein.[51,59,60]

Based on these data, a model for the role of the Jα-helix of YcgF during signal transduction is proposed: In the dark-adapted state the C-terminal α-helix interacts with the BLUF domain and moves upon illumination relative to the domain surface, similar to the Jα-helix of LOV2.[40] The reoriented BLUF Jα-helix could thereby affect the EAL domain's activity either by controlling access to the c-di-GMP binding site or by changing its dimeric association,[31] as EAL domains can dimerize as exemplified by the N-terminal EAL domain of YkuI from *B. subtilis* (2BAS).

Conversion between light- and dark-adapted states appears to be rather complex in the YcgF BLUF domain, as indicated by the heterogeneous distribution of half-lives in time-dependent NMR spectra. The heterogeneous recovery of the dark-adapted state indicates a hysteresis effect as observed before for LOV2[50] and PYP.[51] This heterogeneity does not contradict the UV/Vis, ^{31}P and ^{1}H NMR spectroscopically determined half-lives of the light-adapted state. Here, the UV/Vis values reflecting the chemical environment of the isoalloxazine chromophore correlate with the fastest NMR-derived half-lives, similar to LOV2.[50] The ^{31}P NMR values correlate with the average ^{1}H NMR lifetimes, and the reorientation of the Jα-helix correlates with the slowest ^{1}H NMR lifetimes of the FMN containing BLUF photoreceptor. This finding indicates that the YcgF BLUF domain might recover into the dark-adapted state starting with local changes in the isoalloxazine environment that propagate towards the photoreceptor surface and its interface with the Jα-helix.

Conclusions

The global structural changes occurring in the YcgF BLUF domain during light–dark conversion require a huge activation barrier of at least 89 kJ mol^{-1}; similar values were reported before for the stand-alone BLUF domain of Tll0078.[21] This kinetic barrier corresponds to a doubling of the decay rates upon a temperature rise of just 6 K. This temperature dependency might be biologically relevant, as it affects the activity of *E. coli* YcgF as a putative phosphodiesterase. As mentioned before, EAL-class phosphodiesterases hydrolyze c-di-GMP, which is a second messenger that regulates the multicellular behavior of bacteria, and, in particular, the delicate balance between motile and sessile life styles.[33,35,37] Recent results advert a decrease in biofilm formation and raised motility for *E. coli* K12 grown under blue light, whereas this effect is missing in cells grown under red light and in *E. coli* mutants lacking the *ycgF* gene.[38] Under dark conditions, the YcgF BLUF domain exists in its ground state and hence might inhibit the EAL domain. In this case, the increased c-di-GMP concentration would trigger biofilm formation by *E. coli*. At ambient temperatures and under blue light, the EAL domain would be activated by the light-adapted BLUF domain to hydrolyze the second messenger thus causing enhanced mobility.[38] At lower temperatures the light-adapted state of the YcgF BLUF domain is further stabilized, thus causing an even stronger bias to motile life style.

Interestingly, various bacteria, for example *Burkholderia xenovorans*, possess LOV-domain-coupled EAL and GGDEF domains;[38,61] this suggests the existence of similar mechanisms between the respective photoreceptor domain and c-di-GMP-regulating output domains. Thus, YcgF might play an important role in temperature- and light-dependent regulation of bacterial biofilm formation. Such a coupling between two environmental cues might not be without precedent, since animal and plant cryptochromes have been claimed to represent blue-light-dependent magnetoreceptors.[62–64] From this one may wonder whether *E. coli* YcgF could indeed function as a blue-light-dependent molecular thermometer.

Experimental Section

Reagents and buffers: All chemicals were purchased from Sigma–Aldrich, Merck and Fluka.

Cloning and expression: Using genomic DNA from *E. coli* strain DH5α (Stratagene) and the primers ycgFup 5′-GGC ATA TGG CTA GCC TTA CCA CCC TTA TTT ATC TAG C-3′, ycgF113down 5′-CCG GAA TTC ATT ACC CTT TGT CGA ATA CGG CC-3′ and ycgF137down 5′-CCG GAA TTC ATT ACT CGG TTG CAA GGA CAA AAG-3′ the BLUF domains YcgF-(1–113) and YcgF-(1–137) were amplified by PCR introducing NheI and EcoRI restriction sites. The resultant PCR products were ligated into the pCR®2.1TOPO® vector and subcloned into the pET36b (Novagen) expression vector through the same re-

striction sites, to yield the plasmids pET36-YcgF-(1–113) and pET36-YcgF-(1–137).

The *E. coli* BLUF domains YcgF-(1–113) and YcgF-(1–137) were expressed the in *E. coli* strain BL21(DE3) Gold (Stratagene) in 2 L LB-medium (Luria Bertani) or in ^{15}N isotope labelled rich growth OD2 media (Silates) containing kanamycin (35 μg mL^{-1}) at 37 °C. After induction with IPTG (1 mM) at OD_{595} 0.5–0.6, cells were harvested after 2 h, resuspended in buffer I (20 mM Tris/HCl, pH 8.0 and 200 mM NaCl) and disrupted in buffer I supplemented with lysozyme (1.2 mg mL^{-1}), EDTA (1 mM), PMSF (0.6 mM), LDAO (3%, *w/v*) and DNase I (24 μg mL^{-1}) for the isolation of inclusion bodies. The inclusion bodies were washed three times with buffer I containing EDTA (1 mM), PMSF (0.3 mM), LDAO (0.75%, *w/v*), one more time with this buffer lacking LDAO and finally twice with ddH_2O.

Refolding and reconstitution with flavin chromophores: The inclusion bodies were solubilized in buffer I supplemented with GdnHCl (6 M), DTT (0.1 M). The denatured BLUF domains were dialyzed with a 7.5-fold excess of FAD or a 15-fold excess of FMN or riboflavin, respectively, against Tris/HCl (20 mM, pH 8.0) for 1.5 days by using a SnakeSkin dialysis tube with a MW cutoff of 3.5 kDa (Pierce). The soluble fractions were collected after centrifugation at 1500 g for 10 min, at 4 °C.

Purification and determination of protein-to-chromophore ratios: Solutions comprising YcgF-(1–113) or YcgF-(1–137) were concentrated with an anion exchanger Q-Sepharose Fast Flow (GE Healthcare) by eluting with a minimal volume of Tris/HCl (10 mM, pH 8.0), NaCl (1 M). The YcgF BLUF domains were purified by gel filtration using a Superdex 200 XK 16/70 column (GE Healthcare) equilibrated before with Tris/HCl (20 mM, pH 8.0). The apparent molecular mass of the YcgF BLUF domain was estimated by the use of gel filtration calibration kits (GE Healtcare). Concentration was completed again with a Q-Sepharose Fast Flow column, and the YcgF fragments were eluted with with buffer I or centrifuge filter devices (Sartorius AG). The purified BLUF domains were stored at −20 °C.

To identify the protein-to-chromophore ratios, the BLUF domain concentrations were determined with the BCA assay[65] before heat denaturing the protein in SDS (0.8%, *w/v*), HCl (0.1 M) for 15 min at 65 °C.[44] Concentrations of the free flavin chromophores were determined by measuring their absorption and using specific extinction coefficients estimated for the present buffer conditions (FAD: $\varepsilon_{450} = 10\,077\ M^{-1}\,cm^{-1}$; FMN: $\varepsilon_{448} = 10\,655\ M^{-1}\,cm^{-1}$; riboflavin: $\varepsilon_{448} = 9763\ M^{-1}\,cm^{-1}$[66]).

Spectroscopy: For UV/Vis spectroscopy, a HP 8453 diode array spectrometer (Hewlett Packard) was used. The absorption spectra of the BLUF domains YcgF-(1–113) and YcgF-(1–137) with concentrations between 13 and 38 μM were measured in buffer I in the range of 190–1100 nm at 291 K. Dark spectra were recorded after incubating the BLUF domains on ice for 2 h in the dark. Before recording the light-adapted spectra the *E. coli* BLUF domains were illuminated for 1 min with a commercial slide projector containing a 250 W lamp type 64655 (Osram).

Half-lives for the regeneration of the dark-adapted state were investigated on a J-810 spectropolarimeter (Jasco) with a Jasco PTC-423S Peltier type temperature control system using a quartz cell (Hellma) with a pathlength of 1 mm and both BLUF domains in concentrations between 30 and 75 μM. Kinetic experiments were performed between 280 and 297 K. Prior to the start of the kinetic experiment, the samples were illuminated with a Philips TLD 58W/25 lamp for 90 s at RT. Using the interval scan measurement modus every 120 or 300 s the absorption values at 503 and 504 nm were recorded during a period of 2 h or 3 h, respectively. Half-lives were calculated from the time-dependent datasets using the mono-exponential decay functions of Origin (OriginLab Corporation).

CD-spectroscopic measurements were recorded on the same instrument using a quartz cell (Hellma) with a pathlength of 1 mm. The BLUF domain concentrations were between 8 and 15 μM. The CD spectra were recorded at 20 °C and 95 °C in the range of 190 nm to 280 nm. The melting curves were carried out at 207 nm by heating the protein solution by 2 °C min^{-1} from 20 to 95 °C and cooled down after 10 s with the same rate to 20 °C.

^{1}H detecting NMR experiments were carried out on 800 or 600 MHz spectrometers (Bruker) using a z-axis gradient, 5 mm TXI-HCN cryogenic probe or a 5 mm TXI-HCN probe without gradients. Standard $^{1}H,^{15}N$ HSQC experiments were carried out on a Bruker 600 MHz spectrometer, equipped with a 5 mm HCN cryogenic probe and a *z*-axis gradient. ^{31}P NMR experiments were run either on an AV 600 MHz spectrometer (Bruker) equipped with a 5 mm TXI-HCP cryogenic probe or on an AV 500 MHz spectrometer (Bruker) equipped with a 5 mm QF-HP cryogenic probe. All samples were dissolved in Tris/HCl (20 mM, pH 8.0), NaCl (1 M), D_2O (10%). ^{1}H chemical shifts were referenced directly to 3-(trimethylsilyl)-1-propane-sulfonic acid sodium salt (Sigma) at 0.015 ppm, whereas ^{15}N was referenced indirectly and ^{31}P chemical shifts were referenced externally to phosphoric acid (85%) at 0.00 ppm. Proton kinetic experiments were performed at five different temperatures (280–297 K) in a pseudo two-dimensional manner, with 300 μM protein concentration and a time resolution of approx. 2 min per data point. $^{1}H,^{15}N$ HSQC spectra were recorded at 291 K using a 700 μM sample with 2 K data points and eight scans average per FID. Proton-decoupled ^{31}P detected kinetic measurements were performed analogously to the proton experiments using a 1.5 mM protein concentration at 291 K only. Prior to the start of the experiment, the samples were illuminated with a 200 W He-Xe lamp emitting light between 300 nm and 450 nm for 10 s to 30 s on ice outside the spectrometer. The NMR spectra were recorded with the software xwinnmr version 3.5 (Bruker) and further processed and analyzed using TOPSPIN version 1.3 (Bruker Biospin) and CARA. The decay and build-up of single peaks were analyzed using SigmaPlot (Systat Software Inc.) by fitting time-dependent peak intensities to three parameter monoexponential functions.

Acknowledgements

Special thanks go to Manuel Maestre Reyna for recording kinetics, Petra Gnau for cloning and Stephan Kiontke for his helpful assistance in purifying both YcgF BLUF domain variants. We thank Helena Kovacs (Bruker Fällanden, Switzerland) for access to H,P cryogenic NMR probes. This work was supported by the European Commission (EU-NMR), the State of Hessen (BMRZ), Deutsche Forschungsgemeinschaft (ES152/4) and the Fonds der Chemischen Industrie.

Keywords: biofilms · BLUF domain · flavins · Jα-helix · NMR spectroscopy · photochemistry

[1] K. J. Hellingwerf, *J. Photochem. Photobiol. B* **2000**, *54*, 94–102.
[2] M. A. van der Horst, K. J. Hellingwerf, *Acc. Chem. Res.* **2004**, *37*, 13–20.
[3] M. Gomelsky, G. Klug, *Trends Biochem. Sci.* **2002**, *27*, 497–500.

[4] M. Iseki, S. Matsunaga, A. Murakami, K. Ohno, K. Shiga, K. Yoshida, M. Sugai, T. Takahashi, T. Hori, M. Watanabe, *Nature* **2002**, *415*, 1047–1051.
[5] J. S. Grinstead, S. T. Hsu, W. Laan, A. M. Bonvin, K. J. Hellingwerf, R. Boelens, R. Kaptein, *ChemBioChem* **2006**, *7*, 187–193.
[6] B. J. Kraft, S. Masuda, J. Kikuchi, V. Dragnea, G. Tollin, J. M. Zaleski, C. E. Bauer, *Biochemistry* **2003**, *42*, 6726–6734.
[7] S. Masuda, C. E. Bauer, *Cell* **2002**, *110*, 613–623.
[8] W. Laan, M. A. van der Horst, I. H. van Stokkum, K. J. Hellingwerf, *Photochem. Photobiol.* **2003**, *78*, 290–297.
[9] W. Laan, T. Bednarz, J. Heberle, K. J. Hellingwerf, *Photochem. Photobiol. Sci.* **2004**, *3*, 1011–1016.
[10] S. Masuda, K. Hasegawa, T. A. Ono, *Biochemistry* **2005**, *44*, 1215–1224.
[11] S. Masuda, K. Hasegawa, T. A. Ono, *FEBS Lett.* **2005**, *579*, 4329–4332.
[12] M. Gauden, S. Yeremenko, W. Laan, I. H. van Stokkum, J. A. Ihalainen, R. van Grondelle, K. J. Hellingwerf, J. T. Kennis, *Biochemistry* **2005**, *44*, 3653–3662.
[13] S. Anderson, V. Dragnea, S. Masuda, J. Ybe, K. Moffat, C. Bauer, *Biochemistry* **2005**, *44*, 7998–8005.
[14] W. Laan, M. Gauden, S. Yeremenko, R. van Grondelle, J. T. Kennis, K. J. Hellingwerf, *Biochemistry* **2006**, *45*, 51–60.
[15] A. Jung, T. Domratcheva, M. Tarutina, Q. Wu, W. H. Ko, R. L. Shoeman, M. Gomelsky, K. H. Gardner, I. Schlichting, *Proc. Natl. Acad. Sci. USA* **2005**, *102*, 12350–12355.
[16] P. Zirak, A. Penzkofer, T. Schiereis, P. Hegemann, A. Jung, I. Schlichting, *J. Photochem. Photobiol. B* **2006**, *83*, 180–194.
[17] K. Hasegawa, S. Masuda, T. A. Ono, *Plant Cell Physiol.* **2005**, *46*, 136–146.
[18] K. Okajima, S. Yoshihara, Y. Fukushima, X. Geng, M. Katayama, S. Higashi, M. Watanabe, S. Sato, S. Tabata, Y. Shibata, S. Itoh, M. Ikeuchi, *J. Biochem.* **2005**, *137*, 741–750.
[19] K. Hasegawa, S. Masuda, T. A. Ono, *Biochemistry* **2004**, *43*, 14979–14986.
[20] S. Masuda, K. Hasegawa, A. Ishii, T. A. Ono, *Biochemistry* **2004**, *43*, 5304–5313.
[21] Y. Fukushima, K. Okajima, Y. Shibata, M. Ikeuchi, S. Itoh, *Biochemistry* **2005**, *44*, 5149–5158.
[22] A. Kita, K. Okajima, Y. Morimoto, M. Ikeuchi, K. Miki, *J. Mol. Biol.* **2005**, *349*, 1–9.
[23] S. Ito, A. Murakami, K. Sato, Y. Nishina, K. Shiga, T. Takahashi, S. Higashi, M. Iseki, M. Watanabe, *Photochem. Photobiol. Sci.* **2005**, *4*, 762–769.
[24] P. Zirak, A. Penzkofer, T. Schiereis, P. Hegemann, A. Jung, I. Schlichting, *Chemical Physics* **2005**, *315*, 142–154.
[25] M. Gauden, J. S. Grinstead, W. Laan, I. H. van Stokkum, M. Avila-Perez, K. C. Toh, R. Boelens, R. Kaptein, R. van Grondelle, K. J. Hellingwerf, J. T. Kennis, *Biochemistry* **2007**, *46*, 7405–7415.
[26] M. Gauden, I. H. van Stokkum, J. M. Key, D. Luhrs, R. van Grondelle, P. Hegemann, J. T. Kennis, *Proc. Natl. Acad. Sci. USA* **2006**, *103*, 10895–10900.
[27] V. Dragnea, M. Waegele, S. Balascuta, C. Bauer, B. Dragnea, *Biochemistry* **2005**, *44*, 15978–15985.
[28] M. Unno, S. Masuda, T. A. Ono, S. Yamauchi, *J. Am. Chem. Soc.* **2006**, *128*, 5638–5639.
[29] T. Domratcheva, B. L. Grigorenko, I. Schlichting, A. V. Nemukhin, *Biophys. J.* **2008**, *94*, 3872–3879.
[30] S. Rajagopal, J. M. Key, E. B. Purcell, D. J. Boerema, K. Moffat, *Photochem. Photobiol.* **2004**, *80*, 542–547.
[31] Y. Nakasone, T. A. Ono, A. Ishii, S. Masuda, M. Terazima, *J. Am. Chem. Soc.* **2007**, *129*, 7028–7035.
[32] K. Hasegawa, S. Masuda, T. A. Ono, *Biochemistry* **2006**, *45*, 3785–3793.
[33] A. J. Schmidt, D. A. Ryjenkov, M. Gomelsky, *J. Bacteriol.* **2005**, *187*, 4774–4781.
[34] R. Tamayo, A. D. Tischler, A. Camilli, *J. Biol. Chem.* **2005**, *280*, 33324–33330.
[35] U. Jenal, J. Malone, *Annu. Rev. Genet.* **2006**, *40*, 385–407.
[36] U. Romling, M. Gomelsky, M. Y. Galperin, *Mol. Microbiol.* **2005**, *57*, 629–639.
[37] R. Tamayo, J. T. Pratt, A. Camilli, *Annu. Rev. Microbiol.* **2007**, *61*, 131–148.
[38] M. A. van der Horst, J. Key, K. J. Hellingwerf, *Trends. Microbiol.* **2007**, *15*, 554–562.
[39] W. D. Hoff, A. Xie, I. H. Van Stokkum, X. J. Tang, J. Gural, A. R. Kroon, K. J. Hellingwerf, *Biochemistry* **1999**, *38*, 1009–1017.
[40] S. M. Harper, L. C. Neil, K. H. Gardner, *Science* **2003**, *301*, 1541–1544.
[41] A. Losi, *Photochem. Photobiol.* **2007**, *83*, 1283–1300.
[42] H. Yuan, S. Anderson, S. Masuda, V. Dragnea, K. Moffat, C. Bauer, *Biochemistry* **2006**, *45*, 12687–12694.
[43] P. Hazra, K. Inoue, W. Laan, K. J. Hellingwerf, M. Terazima, *Biophys. J.* **2006**, *91*, 654–661.
[44] O. Kleiner, J. Butenandt, T. Carell, A. Batschauer, *Eur. J. Biochem.* **1999**, *264*, 161–167.
[45] A. Jung, J. Reinstein, T. Domratcheva, R. L. Shoeman, I. Schlichting, *J. Mol. Biol.* **2006**, *362*, 717–732.
[46] P. Zirak, A. Penzkofer, C. Lehmpfuhl, T. Mathes, P. Hegemann, *J. Photochem. Photobiol. B* **2007**, *86*, 22–34.
[47] L. Blanchard, C. N. Hunter, M. P. Williamson, *J. Biomol. NMR* **1997**, *9*, 389–395.
[48] J. Kikuchi, T. Asakura, K. Hasuda, T. Ito, K. Ohwaku, H. Araki, M. P. Williamson, *J. Biochem. Biophys. Methods* **2000**, *42*, 35–47.
[49] S. J. Perkins, K. Wuthrich, *J. Mol. Biol.* **1980**, *138*, 43–64.
[50] S. M. Harper, L. C. Neil, I. J. Day, P. J. Hore, K. H. Gardner, *J. Am. Chem. Soc.* **2004**, *126*, 3390–3391.
[51] G. Rubinstenn, G. W. Vuister, F. A. Mulder, P. E. Dux, R. Boelens, K. J. Hellingwerf, R. Kaptein, *Nat. Struct. Biol.* **1998**, *5*, 568–570.
[52] M. E. Van Brederode, W. D. Hoff, I. H. Van Stokkum, M. L. Groot, K. J. Hellingwerf, *Biophys. J.* **1996**, *71*, 365–380.
[53] A. Akmal, V. Munoz, *Proteins* **2004**, *57*, 142–152.
[54] H. Durr, M. Salomon, W. Rudiger, *Biochemistry* **2005**, *44*, 3050–3055.
[55] S. Crosson, K. Moffat, *Proc. Natl. Acad. Sci. USA* **2001**, *98*, 2995–3000.
[56] S. M. Harper, J. M. Christie, K. H. Gardner, *Biochemistry* **2004**, *43*, 16184–16192.
[57] S. Masuda, Y. Tomida, H. Ohta, K. Takamiya, *J. Mol. Biol.* **2007**, *368*, 1223–1230.
[58] C. L. Partch, M. W. Clarkson, S. Ozgur, A. L. Lee, A. Sancar, *Biochemistry* **2005**, *44*, 3795–3805.
[59] P. Dux, G. Rubinstenn, G. W. Vuister, R. Boelens, F. A. Mulder, K. Hard, W. D. Hoff, A. R. Kroon, W. Crielaard, K. J. Hellingwerf, R. Kaptein, *Biochemistry* **1998**, *37*, 12689–12699.
[60] C. Bernard, K. Houben, N. M. Derix, D. Marks, M. A. van der Horst, K. J. Hellingwerf, R. Boelens, R. Kaptein, N. A. van Nuland, *Structure* **2005**, *13*, 953–962.
[61] S. Crosson, S. Rajagopal, K. Moffat, *Biochemistry* **2003**, *42*, 2–10.
[62] M. Ahmad, P. Galland, T. Ritz, R. Wiltschko, W. Wiltschko, *Planta* **2007**, *225*, 615–624.
[63] M. Liedvogel, K. Maeda, K. Henbest, E. Schleicher, T. Simon, C. R. Timmel, P. J. Hore, H. Mouritsen, *PLoS ONE* **2007**, *2*, e1106.
[64] H. Mouritsen, T. Ritz, *Curr. Opin. Neurobiol.* **2005**, *15*, 406–414.
[65] P. K. Smith, R. I. Krohn, G. T. Hermanson, A. K. Mallia, F. H. Gartner, M. D. Provenzano, E. K. Fujimoto, N. M. Goeke, B. J. Olson, D. C. Klenk, *Anal. Biochem.* **1985**, *150*, 76–85.
[66] J. Koziol, *Methods Enzymol.* **1971**, *18*, 253–285.
[67] D. Apiyo, P. Wittung-Stafshede, *Protein Sci.* **2002**, *11*, 1129–1135.
[68] C. L. Higgins, B. K. Muralidhara, P. Wittung-Stafshede, *Protein Pept. Lett.* **2005**, *12*, 165–170.

Received: April 24, 2008
Published online on September 12, 2008

